Lighting up the Senses: FM1-43 Loading of Sensory Cells through Nonselective Ion Channels

Jason R. Meyers,[1]* Richard B. MacDonald,[3]* Anne Duggan,[5,6] David Lenzi,[2] David G. Standaert,[4,7] Jeffrey T. Corwin,[2] and David P. Corey[5,6]

[1]Neuroscience Graduate Program and [2]Departments of Otolaryngology-Head and Neck Surgery and Neuroscience, School of Medicine, University of Virginia, Charlottesville, Virginia 22908, [3]Program in Speech and Hearing Sciences, Health Sciences and Technology Program, Massachusetts Institute of Technology, Boston, Massachusetts 02139, Departments of [4]Neurology and [5]Neurobiology, Harvard Medical School, Boston, Massachusetts 02115, and Howard Hughes Medical Institute, [6]Neurosurgery Service, and [7]Neurology Service, Massachusetts General Hospital, Boston, Massachusetts 02114

We describe a novel mechanism for vital fluorescent dye entry into sensory cells and neurons: permeation through ion channels. In addition to the slow conventional uptake of styryl dyes by endocytosis, small styryl dyes such as FM1-43 rapidly and specifically label hair cells in the inner ear by entering through open mechanotransduction channels. This labeling can be blocked by pharmacological or mechanical closing of the channels. This phenomenon is not limited to hair cell transduction channels, because human embryonic kidney 293T cells expressing the vanilloid receptor (TRPV1) or a purinergic receptor ($P2X_2$) rapidly take up FM1-43 when those receptor channels are opened and not when they are pharmacologically blocked. This channel permeation mechanism can also be used to label many sensory cell types *in vivo*. A single subcutaneous injection of FM1-43 (3 mg/kg body weight) in mice brightly labels hair cells, Merkel cells, muscle spindles, taste buds, enteric neurons, and primary sensory neurons within the cranial and dorsal root ganglia, persisting for several weeks. The pattern of labeling is specific; nonsensory cells and neurons remain unlabeled. The labeling of the sensory neurons requires dye entry through the sensory terminal, consistent with permeation through the sensory channels. This suggests that organic cationic dyes are able to pass through a number of different sensory channels. The bright and specific labeling with styryl dyes provides a novel way to study sensory cells and neurons *in vivo* and *in vitro,* and it offers new opportunities for visually assaying sensory channel function.

Key words: **FM1-43; hair cell; vanilloid receptor; purinergic receptor; Merkel cells; DRG; nociceptors; TRP channels; sensory ganglia**

Introduction

The styryl pyridinium dye FM1-43 has been widely used to observe synaptic vesicle recycling. FM1-43 is a nontoxic, fluorescent, cationic dye whose fluorescence increases many fold after partitioning into membrane (Betz et al., 1996; Schote and Seelig, 1998). Extracellularly applied FM1-43 partitions into the outer leaflet of the plasma membrane but does not cross between the membrane leaflets, so internalization and loss of FM1-43 fluorescence have been used to measure membrane uptake and exocytosis, respectively (Betz et al., 1996; Henkel et al., 1996).

Styryl pyridinium dyes such as FM1-43, DASPEI, and 4-Di-2-ASP also label sensory hair cells in the lateral lines and inner ears of vertebrates (Jorgensen, 1989; Balak et al., 1990; Collazo et al., 1994; Nishikawa and Sasaki, 1996; Seiler and Nicolson, 1999; Gale et al., 2001; Meyer et al., 2001). FM1-43 quickly fills the cytoplasm of hair cells, but labels only the plasma membrane in adjacent supporting cells. FM1-43 entry into hair cells has been taken as a measure of endocytosis (Self et al., 1999; Seiler and Nicolson, 1999; Meyer et al., 2001; Griesinger et al., 2002), which is thought to occur via vigorous membrane trafficking at hair cell apical surfaces (Forge and Richardson, 1993; Kachar et al., 1997). However, endocytosed high molecular weight markers are limited to apical endosomes in hair cells, whereas FM1-43 also labels endoplasmic reticulum and mitochondria (Nishikawa and Sasaki, 1996). In addition, rapid entry of FM1-43 is blocked by drugs that block the mechanically gated transduction channels, and the dye can itself act as a permeant blocker of the channels (Nishikawa and Sasaki, 1996; Gale et al., 2001). It has therefore been suggested that styryl dyes may enter hair cells by passing directly through mechanically gated transduction channels at the tips of the stereocilia (Balak et al., 1990; Nishikawa and Sasaki, 1996; Gale et al., 2001).

We found that FM1-43 rapidly entered hair cells through the tips of the stereocilia and that entry was inhibited by closing transduction channels, confirming previous suggestions that the dye passes into hair cells through the transduction channel. We then examined whether dye permeation was a property of other nonselective cation channels, and we found that FM1-43 rapidly accumulated in cells expressing the capsaicin receptor TRPV1 or

Received Jan. 2, 2003; revised March 4, 2003; accepted March 7, 2003.

This work was supported by National Institute on Deafness and Other Communication Disorders Grants R01-DC00200 (J.T.C.) and R01-DC00304 (D.P.C.). J.R.M. is a predoctoral fellow, A.D. was an associate, and D.P.C. is an investigator of the Howard Hughes Medical Institute. We thank Baljit S. Khakh and Henry A. Lester (California Institute of Technology) for the $P2X_2$ clone, Stefan Heller (Massachusetts Eye and Ear Infirmary) for the TRPV1 clone, Heidi L. Rehm and Gwénaëlle S. G. Géléoc [Massachusetts General Hospital (MGH)] for valuable advice and help with dissections, Ellen Lumpkin and David Julius (University of California San Francisco) for examining the $P2X_2$ knock-out mouse, David Hill (University of Virginia) for helping to examine the taste system and for helpful discussions, Christine Kellar-McGandy (MGH) for brain sectioning, and Michael Whalen (MGH) for ventricle injections.

*J.R.M. and R.B. M. contributed equally to this work.

Correspondence should be addressed to Jason R Meyers, MR 4, Room 5148, HSC Box 801392, University of Virginia, Charlottesville, VA 22908. E-mail: jmeyers@virginia.edu.

A. Duggan's present address: Departments of Anesthesiology and Physiology, Northwestern University Institute for Neurosciences, Chicago, IL 60611.

D. Lenzi's present address: Cytokinetics Inc., South San Francisco, CA 94080.

 0270-6474/03/234054-12$15.00/0

the purinergic receptor $P2X_2$ when those channels were stimulated by agonists. Most strikingly, subcutaneous dye injection in mice brightly labeled hair cells, Merkel cells, muscle spindle organs, nociceptors, and taste receptors for at least 2 weeks. The dye also entered through sensory terminals to label neurons of the cranial sensory and dorsal root ganglia and the mesencephalic nucleus of the trigeminal. Dye permeation through ion channels provides novel means for visualizing, identifying, and selecting sensory cells and neurons *in vitro* and *in vivo*, and provides an optical measure of channel function for screening mutations and pharmacological agents that act on channels involved in sensory transduction.

Materials and Methods

Reagents. Dyes, drugs, and enzymes were purchased from the following suppliers: FM1-43, FM3-25, and FM4-64, rhodamine-conjugated lipophilic dextran, AlexaFluor 568 phalloidin, and BAPTA (Molecular Probes, Eugene, OR); AM1-43 (Biotium, Hayward, CA); Advasep-7 (CyDex, Overland Park, KS); bacterial proteases XXVII and XXIV, ATP, pyridoxalphosphate-6-azophenyl-2′,4′-disulfonic acid (PPADS), NaCl, KCl, $CaCl_2$, D-glucose, HEPES, capsaicin, and Ruthenium Red (Sigma, St. Louis, MO); Cell-Tak (Collaborative Biomedical Products, Bedford, MA); DMEM and heat-inactivated bovine serum (Invitrogen, Gaithersburg, MD); and Lipofectamine Plus (Invitrogen, Carlsbad, CA).

Dissection and preparation of bullfrog saccules. Saccules were removed from adult bullfrogs (*Rana catesbeiana;* 4–5 inches) into a low calcium Ringer's solution (LCR) containing (in mM): 140 NaCl, 2 KCl, 0.1 $CaCl_2$, 5 D-glucose, and 5 HEPES). The otolithic membranes were removed with fine forceps after incubation in either protease XXIV (50 μg/ml) for 20 min or subtilisin (50 μg/ml) for 10 min. Unless otherwise noted, loading experiments were done in LCR at room temperature. All animal experiments were performed in accordance with approved protocols at the University of Virginia and Massachusetts General Hospital.

Dissection and culture of mouse cochleas and utricles. Temporal bones were removed from C3H/HeN mice (Charles River, Wilmington, MA) at postnatal day 0 (P0) or P1. Utricles were exposed, and otolithic membranes were removed with 100 μg/ml bacterial protease XXVII for 20 min at room temperature. Cochleae and utricles were affixed to Cell-Tak-treated coverglass and incubated in HEPES-buffered DMEM with 10% heat-inactivated bovine serum at 37°C with 5% CO_2 for 24–48 hr.

Confocal flow chamber. Coverslips with an attached cochlea or utricle were dipped briefly (1 sec) in medium containing 3 μM FM1-43 and placed in a flow chamber. Outflow was removed from the chamber with a peristaltic pump. Confocal images were collected every 2.2 sec using a Bio-Rad (Hercules, CA) MRC-1024. FM1-43 (3 μM) was added to the flow solution at the indicated times.

Model of FM1-43 entry. To model dye entry through the transduction channels into cytoplasm, we supposed that healthy hair cells at their resting potentials have a peak transduction current of 500 pA divided among 50 stereocilia, that transduction channels have a resting open probability of 10% (Shepherd and Corey, 1994), that FM1-43 passes throughout the channels at 20% as well as does Na^+, and that entry is proportional to concentration. We constructed a compartment model of the hair cells in which the cell was divided into 1 μm sections from top to bottom and each section had a cytoplasmic compartment and an intracellular lipid compartment. In addition, the stereocilia had an extracellular lipid compartment accessible from the bath. Dye could diffuse in one dimension in both cytoplasm and lipid and partition into or out of the lipid compartments. We assumed that dye partitions into and out of extracellular and intracellular leaflets of both plasma membranes and organelle membranes with a lipid partition coefficient of 3.2×10^4 (Schote and Seelig, 1998; adjusted for charge screening by divalent cations), that its off rate constant is 0.37/sec (Ryan et al., 1996), that its diffusion constant in aqueous medium is 200 μm^2/sec (like that of fluorescein and small dextrans; Periasamy and Verkman, 1998), and that its diffusion constant in membrane is 1.2 μm^2/sec (Zenisek et al., 2002). The area of lipid membrane within each section was calculated from the dimensions of soma and stereocilia (soma of 6 μm diameter and 16 μm length and stereocilia of 0.4 μm diameter and 8 μm length) and from estimates of membrane in soma organelles relative to plasma membrane (based on electron micrographs of mouse utricular hair cells kindly provided by Dr. Anna Lysakowski, University of Illinois at Chicago, Chicago, IL) as follows: below cuticular plate, 25× plasma membrane area; around the nucleus, 4×; subnuclear, 10×. The lipid concentration was then calculated assuming 1.5×10^6 lipid molecules per square micrometer (Nagle and Tristram-Nagle, 2000). The model, constructed in MatLab 6.5 (Mathworks, Natick, MA), was for the most part constrained by numbers from the literature or from hair cell measurements. Estimates of diffusion constants for dye in cytoplasm vary by twofold to threefold, but the diffusion constant of FM1-43 in lipid has been measured well. The assumption we were least sure of is the 20% relative permeability of FM1-43 (based on the relative permeability of TEA, the +2 charge of FM1-43, and the high permeability of Ca^{2+}), but this just adds a scaling factor. With these parameters, all but ~0.2% of the dye was in the lipid phase and diffused ~200 times slower than in cytoplasm, significantly retarding overall diffusion. Calculated dye concentrations were averaged for the regions representing the stereocilia, the apical cytoplasm and the basal cytoplasm, and were plotted as a function of time.

Temperature dependence of dye loading in bullfrog saccule. To examine the temperature dependence of dye loading, frog saccules were maintained either at 4°C or at 22°C (room temperature). FM1-43 (15 μM), FM3-25 (15 μM), or rhodamine-conjugated lipophilic dextran (200 μg/ml) was added to the medium after 20 min of temperature acclimation, and the saccules were examined 5 min later (FM1-43), or at 15, 60, and 120 min (FM3-25 and dextran).

Bundle blot removal of stereocilia. To remove the hair bundles from hair cells, we followed the "bundle blot" procedure of Shepherd et al. (1989). Briefly, we dissected frog saccules and lightly pressed a ribbon of nitrocellulose paper (~8 × 1 mm; 0.45 μm nitrocellulose membrane; Bio-Rad) against the hair bundles, in four or five regions of the macula. Saccules were then incubated in 2 μM AM1-43 in LCR at room temperature for 3 min, washed in 1 mM Advasep-7 in LCR for 5 min, fixed in 4% formaldehyde for 15 min, and incubated in AlexaFluor568-labeled phalloidin (2 U/ml) to stain hair bundles.

Quantification of FM1-43 uptake. To examine pharmacologic inhibition of the transduction channel, frog saccules were preincubated in one of the following: BAPTA (5 mM for 10 min; $n = 3$), elastase (30 U/ml for 15 min; $n = 4$), and gadolinium (1 mM for 10 min; $n = 5$). Saccules were then incubated in FM1-43 (5 μM) either in saline alone (for BAPTA and elastase-treated saccules), or including the inhibitor (for gadolinium) for 3 min, and washed in saline. A subset of saccules treated with gadolinium was washed for 10 min in saline between gadolinium application and application of FM1-43 in saline alone ($n = 5$). To examine the dependence of loading on external ion concentrations, saccules were incubated in saline containing either no added calcium (in mM: 140 NaCl, 2 KCl, 5 D-glucose, and 5 HEPES), standard LCR, LCR containing 1 mM $CaCl_2$, LCR containing 10 mM $CaCl_2$, or saline with 45 mM K (in mM: 69 NaCl, 45 KCl, 1 $CaCl_2$, 3 D-glucose, and 5 HEPES; $n = 4$), for 1 min before adding FM1-43 (5 μM) to the saline. To quantify fluorescence within hair cells for the calcium series, the average pixel intensity of confocal reconstructions of the entire macula less background fluorescence was averaged for all saccules in a group. For all other treatments, the average pixel intensities of 25 hair cells in four different regions within each macula (100 total hair cells per macula), after subtracting background fluorescence, were averaged to produce a mean hair cell fluorescence for each saccule, and intensities were averaged within groups.

Stream loading of dissociated frog hair cells. To dissociate bullfrog hair cells, we used the method of Assad et al. (1991). Briefly, the inner ear was exposed to LCR containing 1 mM EGTA for 15 min *in situ*. Saccules were then removed from the head, placed into LCR, trimmed, and incubated with 50 μg/ml protease type XXIV for 20 min. The otolithic membranes were removed, and hair cells were flicked out of the epithelia and onto the coverglass bottom of the imaging chamber. A stream of dye was created by pressure ejecting LCR with 2 μM FM1-43 (0.5 μM fluorescein added as a tracer) from a 0.5 μm diameter pipette, while drawing the bath solution into a nearby suction pipette with a 5 μm opening. Pressure and suction were adjusted to minimize the stream diameter. The stream was maneu-

vered by controlling the manipulators holding the outflow and inflow pipettes.

Fluid jet labeling of bullfrog saccules. To mechanically open and close the hair cell transduction channels during dye application, a fluid stream was directed at the sensory epithelium through a 0.1 mm diameter pipette. The stream was changed from a saline solution (LCR plus 4 mM Ca^{2+}) to saline containing 2 μM FM1-43 for 30 sec, and then back to saline, while maintaining constant pressure. The stream was directed across the axis of symmetry of the macula, either toward or away from the nerve, and deflected bundles on both sides of the striola. Images were acquired with a SPOT CCD camera (Diagnostic Instruments, Sterling Heights, MI). Differential interference contrast (DIC) images acquired at a series of focal planes were used to score the orientation of individual bundles on both sides of the striola. Fluorescence images of the same field, but focused within the cell bodies, were used to assess FM1-43 uptake.

Labeling of cell lines transfected with TRPV1 or $P2X_2$. Human embryonic kidney (HEK) 293T cells were transfected using Lipofectamine Plus with plasmids containing either a TRPV1 clone in pcDNA3.1 (obtained from Stefan Heller, Massachusetts Eye and Ear Infirmary) or a $P2X_2$ clone in pcDNA3.1 (obtained from Baljit S. Khakh and Henry A. Lester, California Institute of Technology). Mock transfection cells were treated with Lipofectamine Plus but without plasmid DNA. Cells were allowed at least 24 hr to express the channels before FM1-43 uptake was tested. Unless otherwise specified, experiments were done in mammalian saline (in mM: 130 NaCl, 3 KCl, 2 $MgCl_2$, 2 $CaCl_2$, 10 HEPES, and 10 glucose) at room temperature.

To open the TRPV1 channel, cells were incubated in 0.5 μM capsaicin for 2 min, incubated in 10 μM FM1-43 for 3 min, and washed in 500 μM Advasep-7 to remove free FM1-43. To block TRPV1, cells were incubated as above with the addition of 10 μM Ruthenium Red. To test thermal activation of TRPV1, TRPV1-transfected and mock-transfected cells were incubated at 47°C for 2 min for temperature equilibration, followed by 3 min at 47°C with FM1-43 (10 μM). To open the $P2X_2$ channel, cells were incubated in 20 μM ATP for 2 min, followed by 10 μM FM1-43 with 20 μM ATP for 3 min, followed by washing with 500 μM Advasep-7. To block the P2X receptor, cells were incubated in saline with 100 μM PPADS.

In vivo *uptake of fluorescent dyes.* Mice aged P1 to adult were injected either subcutaneously or intraperitoneally with FM1-43, FM3-25, or AM1-43, at a concentration of 3–5 mg of dye per kilogram of body weight from stocks made up as 1–4 mg/ml in PBS and were killed 1–15 d later. Other neonatal mice (P1–P4) were anesthetized by hypothermia and then received focal injections of AM1-43 into whisker follicles: a glass micropipette was backfilled with 1 mg/ml AM1-43 in PBS, and its tip was pushed along each whisker into the follicle, where a small volume (<1 μl) of dye was injected with a PicoLiter Injector (Harvard Apparatus, Holliston, MA). A third set of mice received stereotactic injections in the left ventricle and extending just above the left ventricle near the corpus callosum. The amount injected was calculated to bring the dye concentration to 10 μM if distributed uniformly throughout the brain.

Mice were killed by CO_2 asphyxiation, and the tissue was fixed after dissection or killed by cardiac perfusion. Mice undergoing cardiac perfusion were anesthetized with urethane (5 ml/kg), exsanguinated with 5 ml of warmed PBS containing 1 mg/ml $NaNO_2$, and then perfused with 5 ml of 4% formaldehyde in PBS.

Tissues were examined at low magnification under a Leica (Nussloch, Germany) MZ FLIII fluorescence dissection microscope, and images were acquired using a CCD camera. Whole mounts or sections of dissected tissues were examined using a Bio-Rad MRC-1024, Bio-Rad Radiance 2000, or Zeiss LSM 510 confocal microscope.

Trigeminal nerve ligation. Neonatal mice (P2–P4) were killed by hypothermia, and the infraorbital branch of the trigeminal nerve that innervates the whiskerpad on the left side of the animal was exposed via a small incision adjacent to the whiskerpad. The nerve was ligated with Vicryl suture (8–0), and the wound was closed with VetBond (3M). Immediately after the ligation, AM1-43 was injected subcutaneously with 5 mg/kg body weight, as described above. To assay the survival of the neurons, some animals were injected with AM1-43 24 hr before the nerve ligation and were not injected after the ligation. After surgery, animals were returned to their mothers for 24 hr, after which they were killed. The trigeminal ganglia and whiskerpads were fixed, sectioned, and examined as described above.

Results

FM1-43 rapidly labels hair cells from the apical pole to the base

To examine the rate of FM1-43 entry into hair cells, we bathed organs from the mouse inner ear in 5 μM FM1-43. A 100 sec application of FM1-43 to a mouse organ of Corti *in vitro* brightly and rapidly labeled the inner and outer hair cells (Fig. 1*A*). Fluorescence first appeared in the hair bundle and moved quickly into the apical cytoplasm. Within 30 sec, it spread to the level of the nucleus, moved into the basal cytoplasm within 60 sec, and accumulated as dye application continued.

Dye spread was quantified during FM1-43 application to mouse utricular hair cells (Fig. 1*B*). As with cochlear hair cells, the bundles of utricular hair cells quickly became bright, and fluorescence progressed below the cuticular plate in 5–10 sec and to the base in <60 sec. After washout, the fluorescence was rapidly lost from the hair bundle but was retained in the cytoplasm (Fig. 1*B,C*). A second dye application produced another transient loading of stereocilia and additional accumulation of fluorescence throughout the cell body (Fig. 1*C*). The initial bright labeling of the hair bundle presumably results from dye partitioning into both the inner and outer leaflets of the stereociliary membrane; indeed, modeling suggests that the dye concentration in the outer leaflet is ~1000 times that in the cytoplasmic leaflet. The rapid decline of fluorescence measured in the bundle during washout is consistent with the departitioning of dye from the outer leaflet back into the media, and the residual bundle fluorescence is comparable to the fluorescence in the cytoplasm (Fig. 1*C*), representing dye that was internalized. The labeling within the cell was persistent; there was no evidence of dye leaving the cells during >6 hr in dye-free medium. In the frog saccule, FM1-43 labeled hair cells with a similar time course and pattern (data not shown), and fluorescence persisted over 3 weeks *in vitro* after a single labeling.

To test whether the pattern and time course of labeling was consistent with FM1-43 entering through the transduction channels at the tips of stereocilia and diffusing through the cytoplasm, we modeled entry of the dye through transduction channels and diffusion throughout the cell (see Materials and Methods). The predicted fluorescence is displayed in Figure 1*D* and is similar to the observed fluorescence.

In the experiments described so far, dye had free access to both apical and basolateral membranes of hair cells. To determine whether the fluorescence descending into the cell bodies resulted from dye entry only at the apical surface, we applied dye to bullfrog saccules that were inverted on a coverglass to seal a volume of dye-free medium at the apical surface (Fig. 1*E*). When FM1-43 was added to the bath for 5 min, the basolateral hair cell membranes were labeled, but their cytoplasmic compartments remained unlabeled (Fig. 1*F*). When the same saccules were then flipped and had dye exposed to the apical surface, the cytoplasmic compartments quickly labeled (Fig. 1*G*), thus rapid labeling of hair cells depends on dye entry through the apical surface.

Rapid FM1-43 entry is not via endocytosis

To determine whether endocytosis could account for the rapid labeling of hair cells, we examined internalization of two larger dyes that are used to follow endocytosis: another styryl dye, FM3–

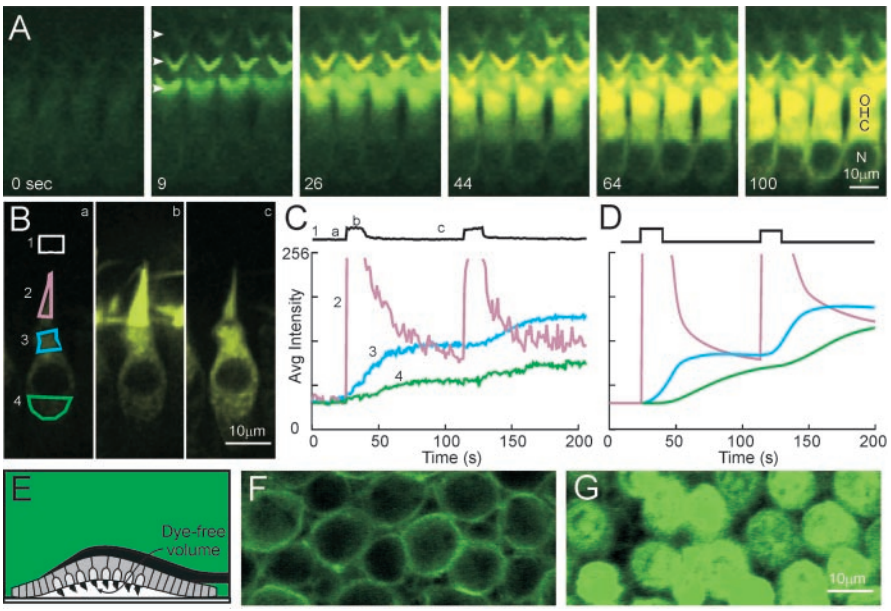

Figure 1. FM1-43 rapidly fills the cytoplasm of auditory and vestibular hair cells, entering from the tops and progressing to the bases of cells. *A,* Confocal time series of FM1-43 labeling in mouse cochlear outer hair cells. Dye spread through the cell within 60 sec of application. Labeling begins with the hair bundles, three rows of which can be seen (arrowheads). Fluorescence then fills the cytoplasm of the outer hair cells (OHC) from the top down, but is excluded from the nucleus (*N*). Four cell bodies from the first row of OHCs are shown. *B,* Confocal images from a time series of FM1-43 labeling of mouse utricular hair cells, before FM1-43 (*a*), during a pulse of FM1-43 (*b*), and during destaining (*c*). Regions for quantification of fluorescence in the medium (1), hair bundle (2), cell apex (3), and cell base (4) in *C* are indicated. *C,* Time course of fluorescence intensity in the regions indicated during two pulses of FM1-43. At the top (1) is the fluorescence of the medium (expanded vertical axis) to indicate the timing of the FM1-43 pulses. Times of the micrographs in *B* are indicated. During FM1-43 application, the fluorescence signal in the bundle rapidly saturated (2); after washout, the bundle signal declined as fluorescence appeared in apical (3), then basal (4) cytoplasm. *D,* Model of fluorescence expected if FM1-43 partitions into and out of the hair bundle plasmalemma and also enters through the tips of stereocilia and diffuses throughout the cytoplasm; regions as in *C* (see Materials and Methods). *E,* Schematic of dye exclusion from hair cell apical surfaces by inverting and sealing a saccule onto coverglass. *F,* Fluorescence micrograph of the apical surface of a saccule positioned as in *E* and incubated for 10 min. The plasma membrane was labeled, but the cytoplasm was unlabeled. *G,* Fluorescence micrograph of a frog saccule unsealed from a coverglass and incubated for 5 min, showing normal labeling of hair cells by FM1-43.

25, and a 10 kDa fluorescent lipophilic dextran (Lippincott-Schwartz and Fambrough, 1986). FM3-25 has the same polar head and fluorescent nuclear domains as FM1-43, but it has two 18-carbon tails, whereas FM1-43 has two 4-carbon tails (Fig. 2*A*).

At 22°C, FM3-25 entered the cytoplasmic compartment of bullfrog saccular hair cells much more slowly than FM1-43. After 15 min, FM3-25 labeled only the plasma membrane (Fig. 2*B*), although by 60 min labeled the cytoplasmic compartment (Fig. 2*D*), whereas FM1-43 brightly labeled the cytoplasmic compartment within 5 min (Fig. 2*C*).

Endocytosis in turtle is blocked by cooling to 4°C (Schaeffer and Raviola, 1978), whereas ion permeation through channels is typically slowed only twofold to threefold (Hille, 1992), allowing temperature dependence to separate endocytotic uptake versus permeation. At 4°C, FM3-25 was restricted to intense labeling of small circular profiles within the apical pericuticular necklace of bullfrog hair cells (Fig. 2*F, inset*), where endocytosis is thought to occur (Hasson et al., 1997; Kachar et al., 1997). Except labeling of the plasma membrane, structures below the apical surface remained unlabeled even after 60 min (Fig. 2*F*). Internalization of a 10 kDa lipophilic dextran was similar: it labeled hair cells only after 1–2 hr at 22°C, and its entry was blocked at 4°C, with the exception of the pericuticular necklace (data not shown). In contrast, FM1-43 internalization was still rapid at 4°C (Fig. 2*E*). All of the dyes showed labeling of the pericuticular necklace, consistent with this being a site of significant apical membrane uptake. The labeling in the pericuticular region by FM3-25 at 4°C suggests that this membrane invagination can occur to a limited degree, even at temperatures that block endocytosis in other species. The pattern of labeling may represent stages of stalled endocytosis or the labeling of fused vesicles whose transport throughout the cell is blocked by the temperature.

Two analogs of FM1-43, FM4-64, which has two 3-carbon tails, and AM1-43, a lysinated, fixable analog with two 4-carbon tails, both labeled hair cells with time courses similar to FM1-43 (data not shown). Thus, rapid cytoplasmic labeling by FM1-43 and styryl dyes of similar size is independent of endocytosis.

FM1-43 enters hair cells through their hair bundles

To test the hypothesis that FM1-43 enters hair cells through their hair bundles, we used nitrocellulose to remove hair bundles (Shepherd et al., 1989) and then incubated the epithelia in AM1-43 for 5 min. Phalloidin labeling revealed bands of bundleless hair cells (Fig. 3*A*, *arrowheads*) that had internalized far less AM1-43 than their neighbors (Fig. 3*B,C*). Cells missing hair bundles were not killed by the procedure, because cells with disrupted membranes avidly take up dye, and the bundleless cells were only dimly labeled, with the residual labeling likely caused by the conventional slow endocytotic uptake of dye. Stereocilia are therefore necessary for the rapid dye entry into the cytoplasm.

To rule out the possibility that hair bundles might be necessary for a dye uptake process that occurs elsewhere on the apical surface, we used a narrow stream to restrict dye application to the stereocilia of isolated hair cells (Fig. 3*J*). When the stream was positioned ~5 μm above the tip of the hair bundle, the hair cells were not fluorescent (Fig. 3*D,K*). As the stream was lowered to the tips of the stereocilia (Fig. 3*E*), the bundle became fluorescent (Fig. 3*F*); within 20 sec, fluorescence spread to the apical cytoplasm (Fig. 3*F,G,K*). Moving the dye stream away from the hair bundle resulted in a loss of bundle fluorescence in 5–10 sec, but the cytoplasmic compartment retained its fluorescence (Fig. 3*H,K*). When the dye stream contacted just the tallest stereocilia, only those stereocilia became fluorescent (Fig. 3*I*). On the other hand, FM1-43 applied to the basolateral surface of hair cells labeled only the plasma membrane and washed out within seconds after the stream was removed, without detectable entry into the cytoplasmic compartment (data not shown). Although dye applied to the tips of the stereocilia is able to diffuse through the outer membrane of the stereocilia to the apical surface, it is unlikely that the observed labeling occurred through apical endocytosis: there is little accumulation of dye in the apical pericuticular region, where endocytosis occurs, and the speed of internalization is more rapid than that of endocytosis. The presence of FM1-43 at the tips of the stereocilia is therefore both necessary and sufficient for its rapid entry into hair cells.

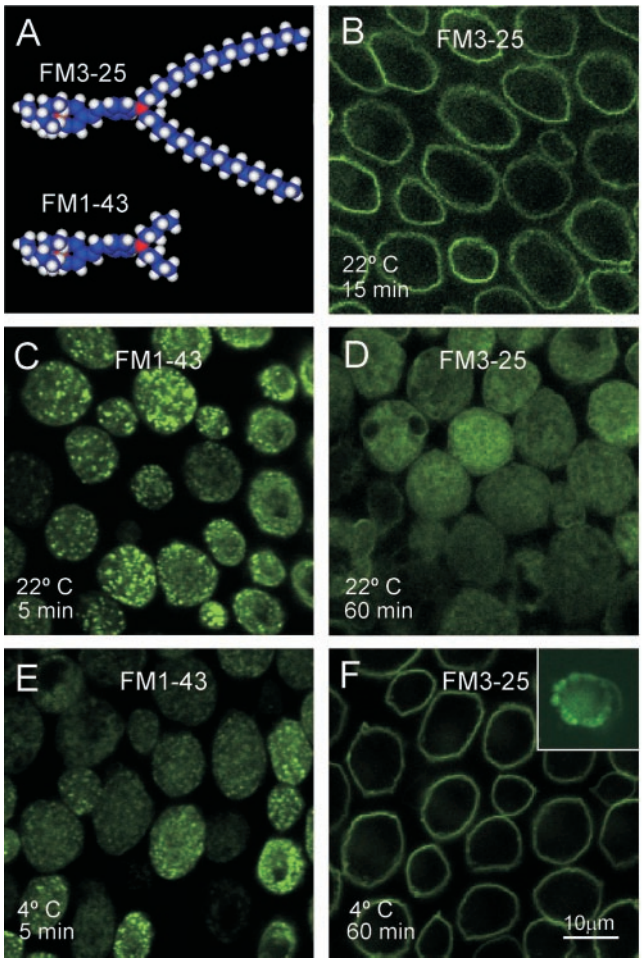

Figure 2. FM1-43 rapidly enters hair cells through a nonendocytotic pathway. *A,* Space-filling models of FM1-43 and FM3-25. *B,* Confocal section of hair cells after a 15 min application of FM3-25 at 22°C; focal plane just below the cuticular plates. The plasma membrane was labeled, but dye was not observed in cytoplasm. *C,* Hair cells after a 5 min application of FM1-43 at 22°C. Cytoplasm was brightly labeled. *D,* After a 60 min application of FM3-25 at 22°C. Fluorescence is present in the cytoplasm. *E,* After a 5 min application of FM1-43 at 4°C. Labeling was similar to but less bright than that at room temperature. *F,* After a 60 min application of FM3-25 at 4°C. Cytoplasmic labeling was blocked. *Inset*, A plane of focus at a the apical surface of a cell. Bright labeling is restricted to a ring around the cuticular plate, the site of apical endocytosis.

FM1-43 enters through the mechanotransduction channels

Because FM1-43 enters through the hair bundles, where the mechanotransduction channels are located, we applied FM1-43 after treatments that affect the transduction channels. Gadolinium, a trivalent cation, blocks the hair cell transduction channel (Kimitsuki et al., 1996) and other stretch-activated channels. Preincubation of frog saccules in 1 mM Gd^{3+} for 10 min completely blocked FM1-43 entry into the cytoplasm of hair cells (Fig. 4*A–C*), but FM1-43 still labeled their plasma membranes (Fig. 4*B, inset*). The block was reversible with 10 min of washout (Fig. 4*C*).

If FM1-43 enters through a channel, then its entry should be dependent on the driving force across the membrane. To change the driving force, we depolarized hair cells to approximately −25 mV by incubation in 45 mM extracellular K^+. The K^+ depolarization reduced entry of FM1-43 to 50% of control (Fig. 4*C*), consistent with passage through a channel.

By chelating calcium, BAPTA cuts the tip links that mechanically couple the transduction channels on adjacent stereocilia, effectively closing the channels (Assad et al., 1991). Treatment of frog saccules with 5 mM BAPTA for 5 min before dye application reduced FM1-43 entry (Fig. 4*C*). Treatment with 32 U/ml elastase also cuts tip links (Osborne and Comis, 1990) and similarly reduced FM1-43 entry (data not shown).

An important test for dye passage through a mechanically gated channel is modulation of its entry by a mechanical stimulus. We simultaneously opened and closed transduction channels in adjacent cells by aiming a fluid jet from a large-bore pipette across the striola, the line in the saccule where hair bundle orientations reverse. Bundles near the pipette were deflected in the negative direction to close transduction channels, whereas adjacent bundles on the far side of the striola were deflected positively to open channels (Fig. 4*E*). Bundles were deflected by 2–3 μm, to hold channels open or closed even after adaptation (Shepherd and Corey, 1994). While maintaining constant velocity, we changed the saline in the fluid jet to one containing 2 μM FM1-43 for 2 min, and then changed back to saline to wash out the dye.

Labeling from the fluid jet extended across a fan-shaped region (Fig. 4*F*). Within this region, hair cells whose bundles were deflected positively (on the far side of the striola) were brightly fluorescent, whereas cells whose bundles were deflected negatively (on the near side) were not. There was a rim of fluorescent hair cells on the negative side of the striola, surrounding the dark cells, where cells were likely bathed in dye but with insufficient velocity or directionality to deflect the bundles.

The line marking the reversal of polarity is not straight, but meanders between oppositely oriented hair bundles. To delineate the points of polarity reversal, we acquired DIC images and scored the polarity of 68 bundles (Fig. 4*G*). The line of polarity reversal ran through the center of the field, but three bundles in the negative region were, in fact, oriented positively (Fig. 4*G, circles*). Internalization of FM1-43 strictly corresponded to the orientation of the hair bundles: all of the hair cells in this field that had positively deflected hair bundles were brightly labeled, whereas none of the cells with negatively deflected bundles were (Fig. 4*H*). Thus, mechanically closing transduction channels is sufficient to block rapid FM1-43 entry into hair cells.

To eliminate the possibility that FM1-43 internalization depends on calcium entry through the transduction channel, which in turn stimulates uptake through another mechanism, we examined internalization under varied calcium concentrations. Above the submicromolar concentrations that break tip-links, FM1-43 entry was not dependent on the external Ca^{2+} concentration, because loading was equivalent in nominally Ca^{2+}-free saline and saline with 0.1 or 1 mM Ca^{2+} (Fig. 4*D*). Loading was reduced in 10 mM Ca^{2+}, which is consistent with Ca^{2+} displacing the divalent FM1-43 from the mouth of the transduction channels or Ca^{2+} decreasing the open probability of the transduction channel (Corey and Hudspeth, 1983). Because direct mechanical closing of the transduction channels and pharmacologic and enzymatic treatments that inhibit transduction are able to block loading of FM1-43 into hair cells, we conclude that FM1-43 passes directly through the transduction channel.

FM1-43 also can pass through TRPV1 and $P2X_2$ ion channels

The vertebrate hair cell transduction channel has not been identified, but a candidate invertebrate mechanoreceptor channel, NOMP-C, has been identified as a member of the TRP superfamily (Walker et al., 2000). To determine whether FM1-43 could permeate a mammalian TRP channel, we investigated the vanilloid receptor TRPV1, which can be opened by capsaicin or by heat (Caterina et al., 1997). HEK293T cells transfected with a

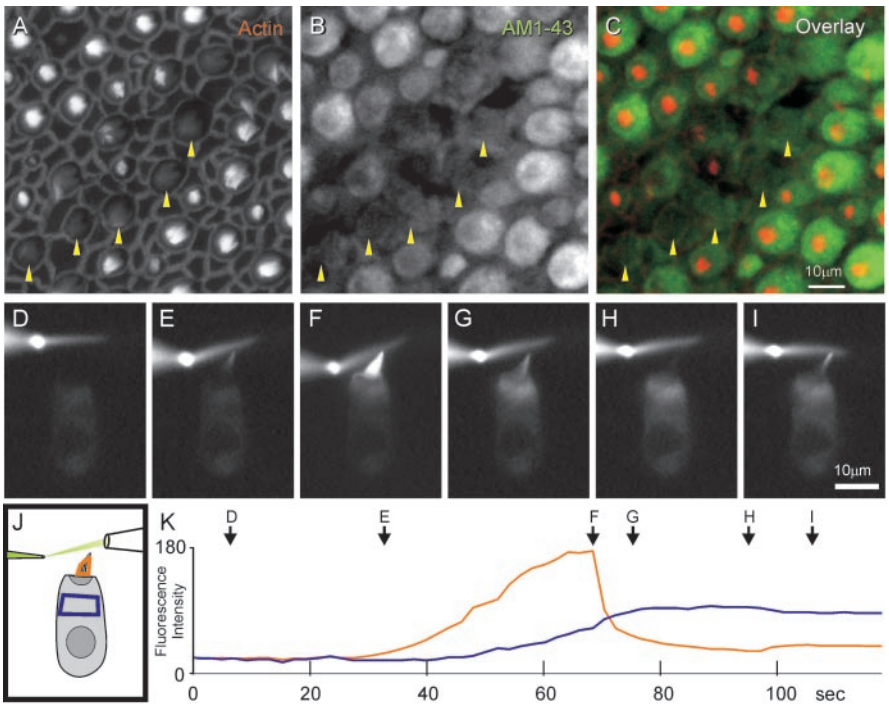

Figure 3. FM1-43 enters bullfrog hair cells through their hair bundles. *A,* Confocal image of phalloidin labeling, at the level of the apical surface. After being blotted with a nitrocellulose strip, a line of hair cells is missing bundles (arrowheads), although their cuticular plates are still intact (fainter disks). *B,* Confocal image of FM1-43 labeling, at a level just below the cuticular plates. *C,* Color overlay of *A* and *B*. Hair cells lacking bundles have much less FM1-43 labeling than adjacent cells with bundles. *D–I,* A series of images from a time series during which FM1-43 was focally applied to the tip of the hair bundle in a narrow stream, with the experimental arrangement in *J*. *E,* Outflow pipette lowered so the stream just grazes the tallest stereocilia. *F,* Stream lowered further to contact the top part of the bundle. Fluorescence appeared in the cytoplasm below the cuticular plate. *G,* Stream raised above the bundle. The bundle began to destain. *H,* The bundle completely destained, but fluorescence is retained in the cytoplasm. *I,* Stream lowered to graze the tallest stereocilia. Only the tallest stereocilia became fluorescent, showing the extent of the dye stream. *J,* Schematic diagram of outflow and inflow pipettes. Regions for quantification of fluorescence within the bundle (red) and apical cell body (blue) are indicated. *K,* Quantification of fluorescence during and after FM1-43 application in the bundle (red) and cell body (blue), with the times of the images *D–I* indicated.

plasmid encoding TRPV1 loaded with FM1-43 within 3 min when 0.5 μM capsaicin was applied (Fig. 5*A*), whereas mock-transfected cells stimulated with capsaicin and TRPV1-transfected cells without capsaicin stimulation did not (Fig. 5*B*). The fraction of cells labeled with FM1-43 in these cultures was comparable to the fraction of cells transfected with a control GFP construct (data not shown). FM1-43 also entered TRPV1 cells held at 47°C for 3 min to open the channels, whereas dye did not enter mock-transfected cells at that temperature (Fig. 5*C*). FM1-43 brightly labeled cells in Ca^{2+}-free saline containing 5 mM BAPTA, indicating that calcium is not a necessary cofactor (data not shown), but loading was blocked by 10 μM Ruthenium Red (Fig. 5*D*), a TRPV1 antagonist (Garcia-Martinez et al., 2000).

When stimulated by ATP, some members of the P2X purinergic receptor family form large pores that allow passage of the cationic dye YO-PRO (Khakh et al., 1999; Virginio et al., 1999). To determine whether a member of this family would also pass FM1-43, we transfected HEK293T cells with $P2X_2$. When $P2X_2$ expressing cells were stimulated with 100 μM ATP for 2 min in the presence of FM1-43, they became brightly fluorescent (Fig. 5*E*), but the entry of FM1-43 through $P2X_2$ was blocked by 100 μM PPADS, a P2X antagonist (Fig. 5*F*). Mock-transfected cells and unstimulated $P2X_2$ cells did not label when exposed to FM1-43 (data not shown).

Sensory receptor cells internalize and retain FM1-43 *in vivo*

Because styryl dyes are capable of permeating through at least three different ion channels (the hair cell transduction channel, $P2X_2$, and TRPV1), we examined the extent of styryl dye permeation through channels by administering FM1-43 or its fixable analog, AM1-43, to neonatal and juvenile mice via a subcutaneous injection of 1–5 mg/kg body weight. Twenty-four hours later, all hair cells in the cochlea (Fig. 6*A–C*) and vestibular organs (Fig. 6*D*) were labeled throughout their cell bodies. The pattern of fluorescence was similar to that produced by direct application of FM1-43 to hair bundles *in vitro*, with granular labeling throughout the cytoplasmic compartment except for the cuticular plate and the nucleus, which remained nonfluorescent.

All hair follicles and especially whisker follicles were brightly fluorescent within 24 hr (Fig. 6*E*). Fluorescence within vibrissae was limited to the Merkel cells and neurites innervating the Merkel cells (Fig. 6*F*). Merkel cells in touch domes within the skin were similarly labeled (Fig. 6*G*). In skeletal muscles, we found bright labeling in the spiral afferent endings of muscle spindle organs, but not within the intrafusal fibers themselves (Fig. 6*H*). Fluorescence could also be seen in the nerve fibers coursing through the cornea (Fig. 6*I*), in nociceptors throughout the animal, for example lining the nasal epithelium (Fig. 6*J*), and in enteric neurons (data not shown). All of these structures have some mechanoreceptive functions, indicating that styryl dye permeation is a property of many mechanosensory cell types.

Not all structures that labeled with AM1-43 were mechanoreceptive. For example, labeling occurred within the kidney (Fig. 6*K*) and in the bladder (data not shown), although this labeling was transient and likely attributable primarily to filtration of the dye from the bloodstream. Bright, persistent labeling was seen within the taste system (Fig. 6*L–P*). AM1-43 labeled fibers throughout the soft palate (Fig. 6*L*) and in the geschmacksstreifen of the hard palate (Fig. 6*M*). Within the tongue all taste papillae were fluorescent, but the pattern of labeling differed among the types of papillae. In fungiform papillae, AM1-43 labeled fibers throughout the papillae but did not label the taste receptor cells (Fig. 6*N,O*). In foliate and circumvallate papillae, in contrast, AM1-43 labeled the taste receptors themselves (Fig. 6*P*), in addition to fibers within the papillae.

When AM1-43 was injected into animals older than ~2 weeks, the labeling of hair cells was reduced or absent, whereas other structures labeled normally. Hair cells dissected from older animals still took up FM1-43 within 1 min, suggesting that as mice mature, the dye loses access to the endolymph bathing hair cell bundles. Subcutaneous injection of FM3-25 failed to label any of the structures above (data not shown). Thus, internalization is a specific property of smaller styryl dyes such as FM1-43.

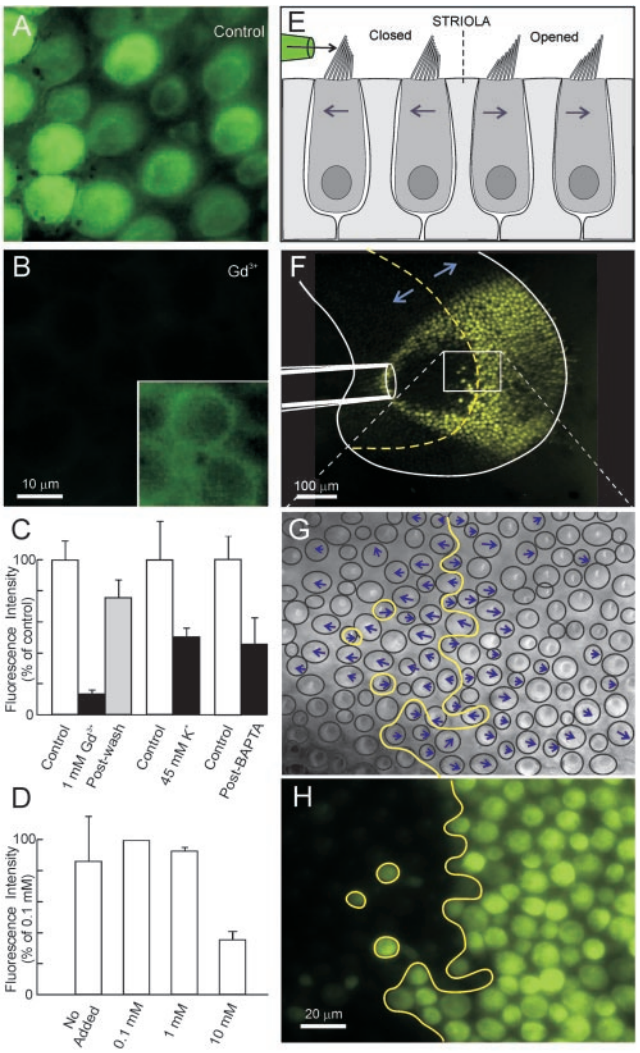

Figure 4. FM1-43 can enter hair cells through the mechanotransduction channel. *A,* Normal loading of frog saccular hair cells incubated in FM1-43. *B,* Hair cells incubated in 1 mM Gd^{3+} before and during FM1-43 loading. *Inset,* Region of *B* intensified to show faint labeling of the plasma membrane. Gd^{3+} blocked internalization of FM1-43. *C,* Quantification of Gd^{3+} block of FM1-43 loading and restoration of loading after Gd^{3+} washout, reduction in loading by depolarization to approximately −25 mV with 45 mM external K^+, and by pretreatment with 5 mM BAPTA to cut tip links (mean ± SEM). *D,* Quantification of FM1-43 loading into frog saccular hair cells in saline with no added Ca^{2+}, 0.1, 1.0 or 10 mM Ca^{2+}. Entry was significantly reduced only by 10 mM Ca^{2+} (mean ± SEM). *E,* Schematic diagram of the stimulus used to open or close transduction channels. Because of the change in bundle orientation at the striola, a fluid jet aimed across the macula closes transduction channels in hair cells on the left side of the striola and opens channels on the right side. *F,* A frog saccule after FM1-43 was blown across the saccule with the fluid jet for 2 min. The saccule and the pipette are outlined in white and the approximate location of the striola in yellow. Cells within the dye stream on the right (positively deflected) side of the striola internalized FM1-43, whereas most cells on the left (negative) side did not. *G,* DIC view of the boxed region in *G* at the plane of the hair bundles. Arrows mark the orientation of 68 hair bundles; a yellow line demarcates the striola. Three hair cells on the left with their bundles oriented toward the right are circled. *H,* Fluorescence micrograph of the field in *H*, taken at the level of the cell bodies. Hair cells with their bundles pushed negatively remained unlabeled, whereas hair cells with their hair bundles pushed positively were brightly labeled with FM1-43.

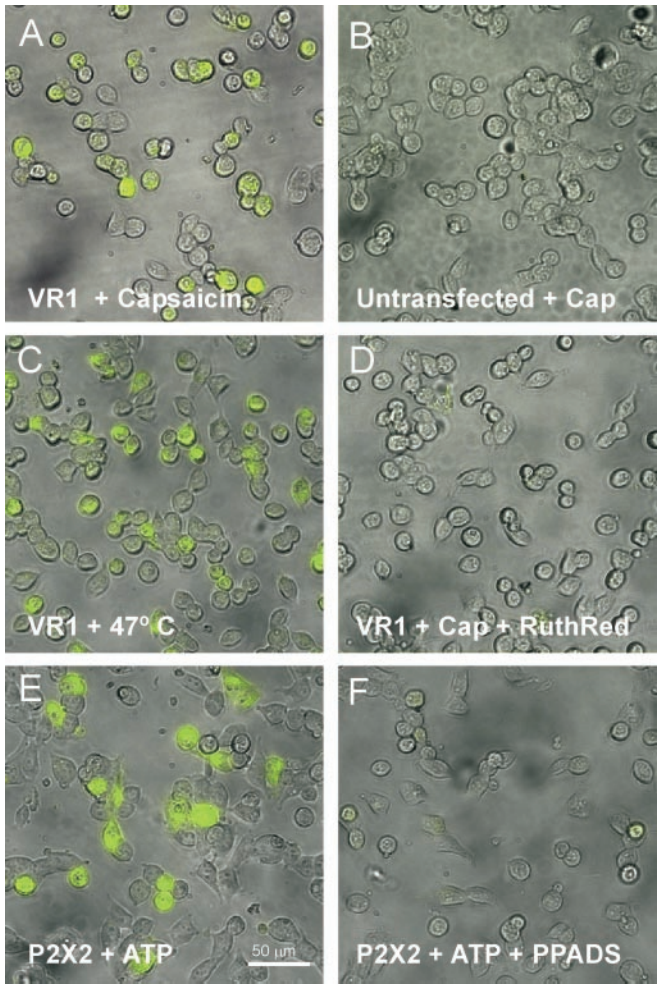

Figure 5. FM1-43 permeates through the capsaicin receptor channel TRPV1 and the ATP receptor channel $P2X_2$. *A,* HEK cells transfected with TRPV1 and exposed to capsaicin (0.5 μM) with FM1-43 (10 μM) for 3 min. *B,* Mock transfected cells exposed to capsaicin and FM1-43. *C,* TRPV1-transfected HEK cells exposed to FM1-43 at 47°C for 3 min. *D,* TRPV1-transfected HEK cells exposed to capsaicin and FM1-43, along with the TRPV1 antagonist Ruthenium Red (10 μM). *E,* HEK cells transfected with $P2X_2$ and exposed to 20 μM ATP with 10 μM FM1-43 for 3 min. *F,* $P2X_2$-transfected HEK cells exposed to ATP and FM1-43, along with the P2X antagonist PPADS (100 μM). Experiments were done at room temperature unless noted.

Primary sensory neurons internalize and retain FM1-43

Also intensely labeled in the injected animals were the cell bodies of primary sensory neurons in the trigeminal (V), geniculate (VII), petrossal (IX), nodose (X), and dorsal root ganglia (DRG) (Fig. 7*A*). The spiral ganglia and vestibular ganglia of the VIIIth nerve were not fluorescent, but those ganglia do not contain primary sensory neurons; instead, they are postsynaptic to the sensory hair cells, which do label with FM1-43. Although the amount of fluorescence in individual neurons varied, most neurons were labeled in every DRG (Fig. 7*B,C*). We did not detect a difference in labeling between large-diameter and small-diameter neurons, indicating that both proprioceptive (large) as well as thermoreceptive and nociceptive (small) neurons internalize the dye. As in hair cells, fluorescence in these neurons was diffuse or granular throughout the cell body, but was excluded from the nucleus (Fig. 7*C*).

Within the brain, only the neurons of the mesencephalic nucleus of the trigeminal (MesV) were brightly fluorescent (Fig. 7*D*, *arrow*). Labeling in MesV neurons was similar to the labeling in sensory neurons of the DRG and cranial ganglia (Fig. 7*E*). The choroid plexus (CP) was fluorescent, and there was weak labeling of blood vessels within the brain and throughout the body. We also saw very faint, punctate fluorescence in motor neurons of the spinal cord and brain, but these neurons were <5% as fluorescent as dorsal root ganglia neurons (data not shown). We wondered whether the absence of label in most CNS neurons resulted from a lack of dye-permeable ion channels or from dye exclusion by the

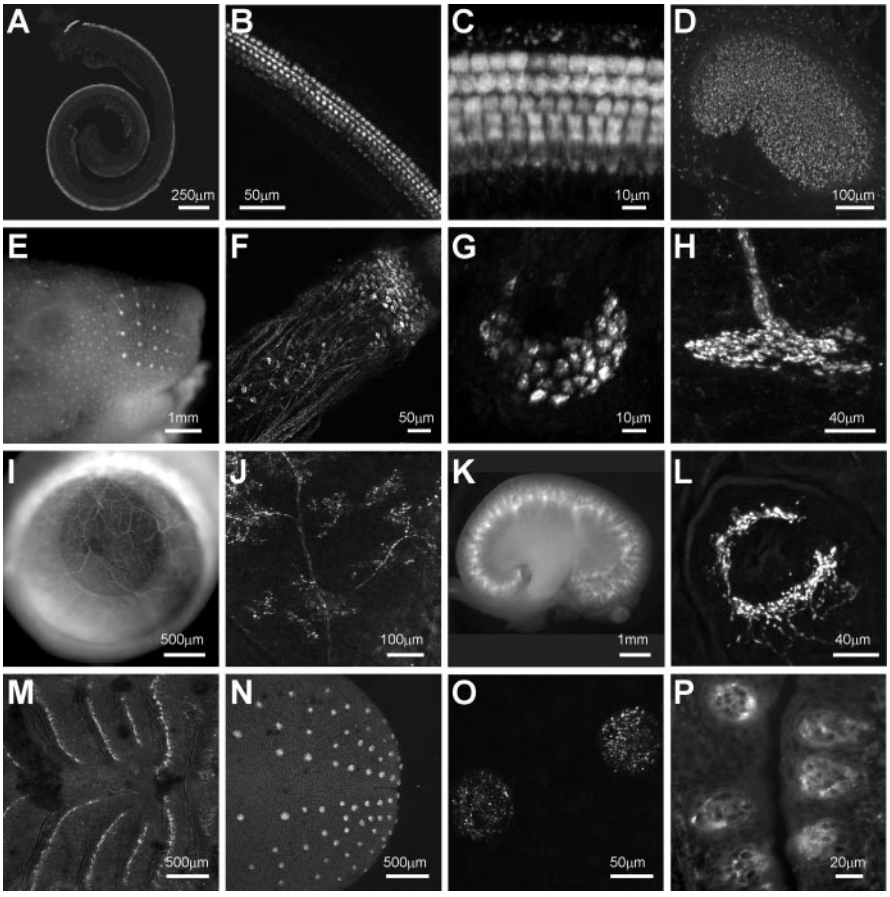

Figure 6. The fixable FM1-43 analog AM1-43 labels many sensory structures after subcutaneous injection into juvenile mice. *A–C,* Cochlear hair cells at increasing magnification. Both inner and outer hair cells were brightly labeled, but other cells in the cochlea were not. *D,* Hair cells in the utricular macula. *E,* Exterior of the head of an injected neonatal mouse. All hair follicles, from snout to tail, were labeled, with the vibrissal follicles most intensely labeled. *F,* The apical half of a single vibrissal follicle. Both Merkel cells and fibers innervating the Merkel cells were labeled. *G,* Merkel cells within a touch dome, just below the surface of back skin. *H,* Spiral fiber in a spindle organ within dissected muscle. *I,* Eye, showing labeling of corneal nociceptive fibers. *J,* Nociceptive fibers from the nasal epithelium. *K,* Cross-section of kidney, with cortical labeling. *L,* Nerve endings within the soft palate. *M,* Labeling in the geschmacksstreifen in the hard palate. *N,* Tongue, with individual taste buds brightly labeled. *O,* Fungiform papillae in tongue. The fibers innervating the taste bud were labeled, but not the taste receptor cells. *P,* Circumvallate papillae in tongue. Taste receptor cells themselves were labeled.

blood–brain barrier, so we injected AM1-43 into and above the left ventricles of two adult mice. The choroid plexus became brightly labeled, and a variety of neurons that project to the injection site were fluorescent; however label in these neurons was less bright than either DRG neurons or mesencephalic trigeminal neurons after subcutaneous injections and resembled label seen with a retrograde tracers, appearing in a subset of organelles close to the axon hillock.

The labeling of the sensory cells and neurons was persistent. Mice that received a single injection of dye still had bright fluorescence throughout the sensory cells and neurons after 2 weeks. Labeling was somewhat less distinct in fine endings, possibly because of transport of labeled membrane back to the cell body. In contrast, motor neurons in the brain and spinal cord lost their already faint labeling after 2 weeks, as did bladder and kidney, suggesting that their labeling was primarily caused by endocytosis or other reversible mechanism rather than permeation into the cells.

FM1-43 enters neurons through sensory terminals

To determine whether labeling in the primary sensory neurons resulted from entry via permeant channels at their sensory endings, AM1-43 was focally applied to the sensory terminals of trigeminal neurons that innervate the vibrissae. Small amounts of dye were injected into individual follicles on one side of the snout in neonatal mice. Twenty-four hours after injection, externally visible fluorescence was limited to the injected vibrissae (Fig. 8*A, arrows*). Internally, a subset of neuronal cell bodies in the ipsilateral trigeminal ganglion were brightly fluorescent (Fig. 8*B*). Thus, dye entering at the sensory terminals was sufficient to label the neurons.

To test whether dye entry at the sensory terminals is necessary for neuronal labeling, the infraorbital branch of the trigeminal nerve, which innervates the vibrissae, was ligated unilaterally just proximal to its entry into the whiskerpad in neonatal mice. AM1-43 was then administered subcutaneously as before. After 24 hr, few neurons were labeled in the nasal portion of the ipsilateral trigeminal ganglion, where the cell bodies of the infraorbital neurons reside (Fig. 8*D,F*), whereas neurons throughout the contralateral ganglion were fluorescent (Fig. 8*C,E*). To ensure that the decrease in labeling had not resulted from death or damage to the neurons in the ganglion, another group of mice was injected with AM1-43, and 24 hr later the infraorbital branch of the trigeminal was ligated. After another 24 hr of recovery, nearly all neurons were labeled in both the ipsilateral and contralateral ganglia, and there was no sign of damage or loss of neurons within the ipsilateral ganglion (Fig. 8*G,H*).

We conclude that the persistent *in vivo* labeling of sensory neurons that occurs after systemic administration of FM1-43 depends dye entry through their sensory terminals with transport back to the cell bodies. This is consistent with labeling in hair cells, where dye rapidly enters the cytoplasmic compartment of the cells only through the sensory apparatus.

Discussion

Permeation of styryl dyes through a channel

Our results are consistent with the ability of styryl dyes to permeate several types of sensory ion channels: the hair cell mechanotransduction channel, the capsaicin receptor, and a purinergic receptor. These results are in contrast to reports that suggest hair cell uptake only by endocytosis (Meyer et al., 2001; Griesinger et al., 2002), but they confirm and extend previous work suggesting passage of FM1-43 through the hair cell transduction channel (Nishikawa and Sasaki, 1996; Gale et al., 2001). The time course of FM1-43 entry into hair cells that we describe here is substantially faster than the labeling reported by Griesinger et al. (2002), suggesting that they were observing only slow endocytosis-mediated uptake and not the fast channel-mediated entry of styryl dyes. Although we are able to see rapid labeling of inner and outer hair cells from the organ of Corti in mice *in vitro*, Griesinger

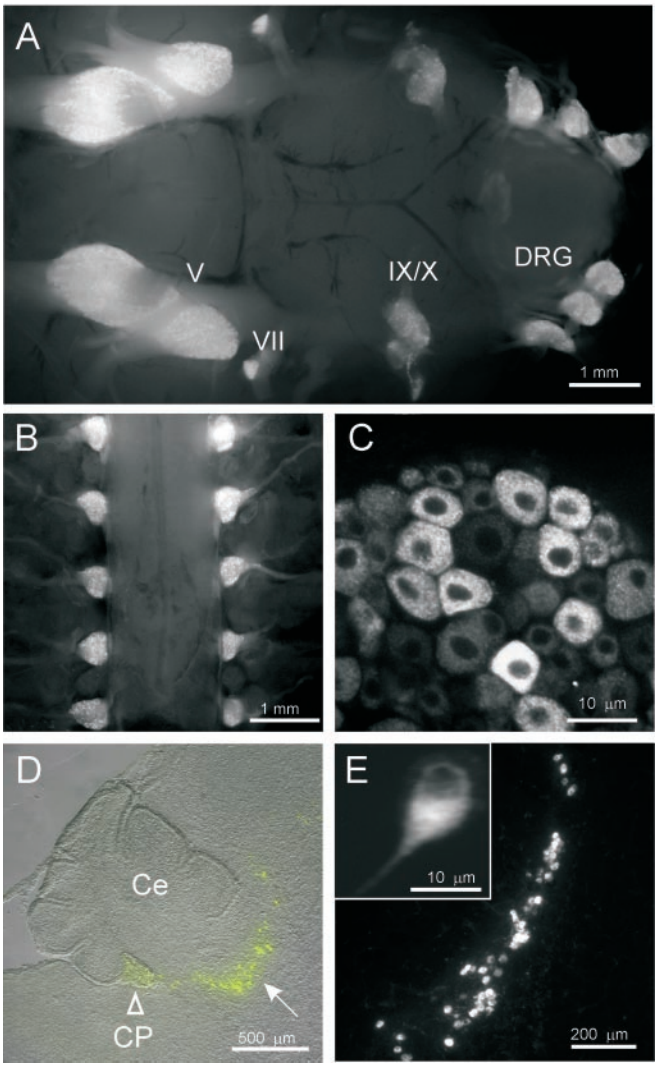

Figure 7. AM1-43 labels primary sensory neurons after systemic injection into juvenile mice. *A,* Brain and initial segment of the spinal cord of a P15 mouse, injected 24 hr before killing. The labels indicate the location of the labeled sensory ganglia. Bottom view; rostral at left. *B,* Dorsal root ganglia throughout the spinal cord label with FM1-43; top view. *C,* Label of neurons within a single dorsal root ganglion; confocal section. Most neurons have accumulated dye, but some are more brightly fluorescent than others. *D,* Sagittal section of brain from an injected mouse; rostral to right. Within the brain, the only brightly labeled neurons were those of the mesencephalic nucleus of the trigeminal (MesV, arrow), located just rostral and ventral of the cerebellum (Ce). The choroid plexus (CP) had lighter fluorescence, and all blood vessels within the brain were faintly fluorescent. *E,* Labeled neurons of MesV in a coronal section of brain. *Inset*, A single neuron in MesV with the cell body and process labeled with FM1-43; label is throughout cytoplasm.

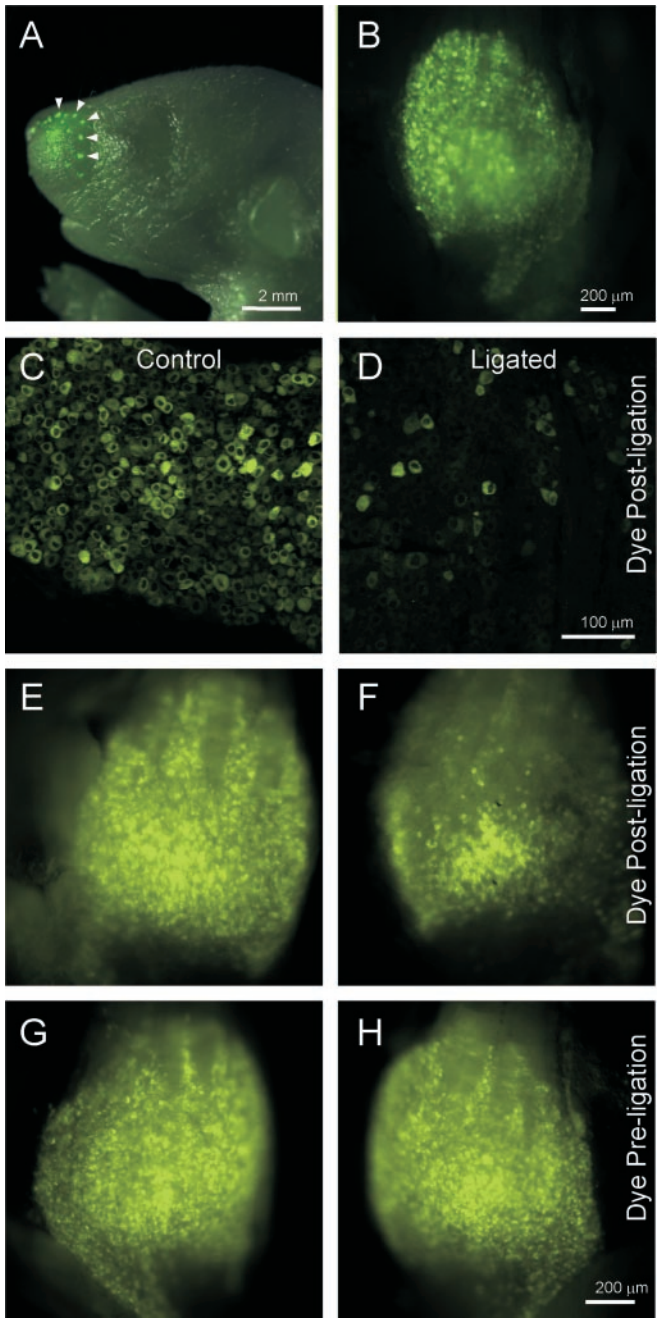

Figure 8. AM1-43 labeling of sensory neurons requires dye at sensory endings. *A,* AM1-43 fluorescence in whisker follicles (arrowheads) 24 hr after injection of dye into individual follicles. *B,* The trigeminal ganglion ipsilateral to the injected follicles. A subset of neurons in the nasal portion of the ganglion (top) was labeled with AM1-43. *C,* Fluorescence in a trigeminal ganglion 24 hr after subcutaneous injection of AM1-43; confocal section. *D,* Fluorescence in the opposite trigeminal ganglion 24 hr after subcutaneous injection of AM1-43 preceded by ligation of the ipsilateral infraorbital branch of the trigeminal nerve. *E, F,* Whole-mount view of control and ligated trigeminal ganglia. Ligation blocked labeling of nasal neurons innervating face (*F*, top) but not posterior neurons (bottom). *G, H,* Fluorescence in whole mounts of trigeminal ganglia 48 hr after subcutaneous injection of AM1-43, and 24 hr after unilateral ligation of the infraorbital nerve. Most neurons within both the unligated and ligated ganglia are labeled.

et al. (2002) saw only endocytotic uptake in an *in situ* organ of Corti preparation from guinea pigs. In our specimens, the organ had been dissected free from surrounding tissue, allowing complete access of the dye to the cells and bundles. Dye access to the tips of the stereociliary bundles may have been limited or the transduction channels may not have been active in their *in situ* preparation. However, their results and ours demonstrate that styryl dyes are able to enter hair cells via a slow endocytotic route. In future analysis of endocytosis-mediated uptake of styryl dyes, care must be taken to ensure that there is not also entry through a dye-permeable channel.

Although our results and those of Gale et al. (2001) are largely complementary, there are a few differences. We see rapid FM1-43 labeling occurring in the bullfrog saccule at 4°C, whereas they saw a block of loading at 4°C in the mouse organ of Corti. The exothermic bullfrog needs to have functional mechanotransduction at depressed body temperatures, and bullfrog transduction channels are known to function at 4°C (Corey and Hudspeth, 1983).

Transduction and adaptation are largely similar between frogs and mice (Holt et al., 1997), although there may be temperature-sensitive aspects of mammalian hair cell physiology that result in a majority of transduction channels being closed at 4°C, such as an adaptation motor that exerts much less tension at that temperature. Gale et al. (2001) also achieved a strong inhibition of FM1-43 entry by using EGTA to sever the tip links in the mouse cochlea, whereas we only found an ~50% reduction using BAPTA and elastase to cut the tip links in the bullfrog saccule. Their inhibition is comparable to the >80% reduction in entry we report with the channel blocker gadolinium and with mechanical closing of the transduction channels. It is possible that our treatments with BAPTA and elastase were not sufficient to completely close all of the transduction channels and that a few surviving tip links or partially opened channels allow a small amount of dye into the cell. The difference in the level of inhibition in our results and reported by Gale et al. (2001) may represent differences in the ability of EGTA, BAPTA, and elastase to sever tip links and close channels or differences in the effects of these treatments between frogs and mice. Taken together, however, our results and those of Gale et al. (2001) are in agreement and highly consistent with the rapid permeation of FM1-43 through the mechanotransduction channels when they are open and not when they are pharmacologically or mechanically closed.

YO-PRO, a cationic dye, can pass through purinergic receptors (Khakh et al., 1999; Virginio et al., 1999), and our evidence suggests that dye permeation through sensory channels is a more general property than was previously thought. It is nonetheless surprising that relatively large cations such as FM1-43 are able to permeate through ion channels. The hair cell transduction channel is a nonselective cation channel, passing monovalent and divalent cations and small organic cations with diameters up to ~0.8 nm (Corey and Hudspeth, 1979; Ohmori, 1985; Lumpkin et al., 1997). For example, the tetraethylammonium ion (TEA; 0.82 nm diameter) permeates, but sixfold less well than Cs^+ (0.36 nm diameter; Ohmori, 1985). Although the molecular weight of FM1-43 is 452, its structure is long and thin, so the polar TEA head group may be the bulkiest part (Fig. 2*A*). Furthermore, FM1-43 is divalent and would have a stronger driving force assisting its entry than the monovalent TEA+. Finally, the size of a molecule is not the only limiting factor for channel permeation. For example, voltage-gated sodium channels, with a narrow selectivity filter (0.3 × 0.5 nm; Hille, 1971), can pass large tetraalkylammonium ions; in fact, larger molecules with more hydrophobic area, such as tetrahexylammonium, permeate better than tetraethylammonium (Huang et al., 2000). Thus, there is precedence for relatively large organic molecules passing through ion channels, and the hydrophobic tails of FM1-43 may aid rather than impede permeation.

Specificity of styryl dye labeling

A systemic injection of styryl dye brightly labels a repeatable subset of cells in the mouse. Because labeling is specific to particular classes of sensory cells and because styryl dyes can permeate through sensory channels, we hypothesize that the labeling observed is caused by permeation through their sensory channels. Consistent with this, loading into trigeminal afferents is dependent on dye entering through sensory terminals. Entry through channels provides a mechanism for reports of styryl dye labeling of Merkel cells and muscle spindles (Nurse and Farraway, 1989; Betz et al., 1996).

Several of the cell types that label with FM1-43 express P2X receptors, including cranial sensory and DRG neurons (Xiang et al., 1998) and hair cells (Housley et al., 1999). P2X receptors are a potential path for dye permeation, but likely do not have a primary role in labeling. In hair cells, mechanical closing of transduction channels inhibited dye entry, suggesting that the bulk of entry is through transduction channels rather than P2X receptors. Furthermore, many cells that express P2X receptors, including spiral and vestibular ganglion neurons, and supporting cells throughout the inner ear (Brandle et al., 1999; Xiang et al., 1999; Jarlebark et al., 2000), do not label with FM1-43. Thus, presence of P2X receptors is not sufficient to permit entry of styryl dyes *in vivo* or *in situ*. Finally, $P2X_2$ knock-out mice take up AM1-43 with a pattern indistinguishable from heterozygote littermates (E. Lumpkin and D. Julius, personal communication). Although P2X channels can form dye-permeable low-selectivity pores *in vitro* (Khakh et al., 1999; Virginio et al., 1999), they may rarely form such pores *in vivo*.

TRPV1 is expressed in dorsal root and cranial neurons, but almost all DRG and trigeminal neurons take up AM1-43, whereas only ~50% of the neurons (those of small and medium diameter) express TRPV1 (Michael and Priestly, 1999). Other related channels, such as TRPV3, expressed in most DRG and trigeminal neurons (Xu et al., 2002), may provide additional means of entry. Because little is known about the transduction channels that underlie proprioception, nociception, and mechanoreception in cells other than hair cells, we cannot say how styryl dyes enter into those cell types. The diverse channels that transduce the various sensory modalities in labeled cells may have similar pore structures that are weakly cation selective and permeable for small styryl dyes. Alternatively, a particular class of permeable sensory channels, such as TRP channels, may be widely expressed in all labeled sensory cells and neurons. FM1-43 permeation into transfected cell lines expressing sensory channels provides a novel assay for identifying the sequences encoding sensory channels in these cell types.

Interestingly, in fungiform papillae, taste receptor cells did not label with AM1-43 (Fig. 6*O*), whereas taste receptor cells were labeled in circumvallate and foliate papillae (Fig. 6*P*). The identification of the channels underlying taste transduction has revealed distinct biases in the distribution of receptor channels and accessory proteins between different taste papillae (for review, see Gilbertson et al., 2000; Margolskee, 2002). For example, the TRP channel, TRPM5, is expressed specifically in a large fraction of taste receptor cells in the foliate and circumvallate papillae of the tongue (Perez et al., 2002; Zhang et al., 2003). FM1-43 uptake in these papillae is similar to the pattern of TRPM5 expression (Fig. 6*P*), and the permeation of FM1-43 through other TRP channels suggests that TRPM5 may be a route of entry for styryl dyes into the taste cells. In contrast, the labeling in the fungiform papillae appears to be limited to small diffuse fibers innervating the papillae, similar to those that have been shown to be TRPV1-immunoreactive, whereas no fungiform taste receptor cells show TRPV1 immunoreactivity (Ishida et al., 2002) or styryl dye labeling. This suggests that the primary mechanism of labeling within the fungiform papillae is through the vanilloid receptor into nociceptive fibers localized in each papillae. Because many of the cell types labeled in our preparation are mechanosensory, it is also intriguing to consider the possibility that some of the cells labeled in the taste system might be osmosensitive stretch receptors, such as might be mediated by TRPV4 (Liedtke et al., 2000).

FM1-43 also labels both Merkel cells and the neurons innervating them. Merkel cells are polarized cells that reside in the basal layer of the epidermis and are innervated by afferents to form a type I Merkel cell–neurite complex. Merkel cells have

dense core vesicles concentrated at the site of innervation and were thus hypothesized to be touch-sensitive mechanoreceptors (Iggo and Muir, 1969). Subsequently, there has been substantial debate on whether Merkel cells or the neurites are the actual mechanoreceptive cells. Merkel cells are excitable, but have not been shown to be mechanosensitive, and the nature of the neurotransmitter in the dense core vesicles is unclear. Attempts to block Ca^{2+} channels in or inhibit synaptic release from Merkel cells have lead to contradictory results (Diamond et al., 1986; Pacitti and Findlater, 1988; Senok and Baumann, 1997), and selective ablation of Merkel cells has been reported both to inhibit (Ikeda et al., 1994) and not to affect (Mills and Diamond, 1995) mechanotransduction. The uptake of styryl dyes by both the Merkel cell and the neurite suggests that both cell types may express nonselective sensory channels. FM1-43 permeation into Merkel cells, which occurs as well in dissected vibrissae *in vitro*, may be used to identify the nature of the permeant channel by analysis of compounds and conditions that block or promote entry of the dye. It is further notable that aminoglycoside antibiotics, which block mechanotransduction in hair cells (Ohmori, 1985), have been reported to inhibit mechanotransduction in type I Merkel cell–neurite complexes, but not in type II neurites, which are not associated with Merkel cells (Baumann et al., 1990). Aminoglycoside sensitivity and the permeability of FM1-43 suggest significant similarities between the mechanoreceptive channels in the touch system and in the inner ear.

Within the brain, only neurons in the mesencephalic nucleus of the trigeminal were brightly fluorescent after systemic administration of AM1-43. These are displaced primary sensory neurons, which innervate proprioceptors in the jaw. Neurons behind the blood–brain barrier did not internalize dye, and even when AM1-43 was injected into the brain, labeling was limited to faint retrograde transport of dye. Efferent neurons, such as motor neurons, would be exposed to AM1-43 at their synaptic terminals, where they have significant vesicle recycling and concomitant cycling of dye (Henkel et al., 1996), yet were $<5\%$ as fluorescent as sensory cells of the DRG, and this faint labeling was not persistent. This supports our conclusion that endocytotic uptake of styryl dyes is not sufficient to produce the characteristic bright, persistent labeling of sensory cells. In summary, styryl labeling corresponds directly to cellular function: central, efferent, and higher order afferent neurons without primary sensory transduction do not label brightly with FM1-43, whereas primary sensory cells and neurons become intensely labeled.

Advantages and applications of styryl dye labeling

Styryl permeation through ion channels provides a novel mechanism for labeling of sensory cells and neurons and has many advantages over other vital labeling techniques. Labeling can be achieved *in vivo* via subcutaneous injection of dye, or *in vitro* in dissected tissue or cultured cells, making it useful for a wide range of applications and allowing comparison of results obtained *in vitro* to those *in vivo*. The technique is very rapid with dye filling cells in <1 min *in vitro* and allowing for systemic distribution within 24 hr *in vivo*.

For FM1-43 taken up by endocytosis, membrane trafficking and exocytosis eventually expose the dye to the extracellular medium, where it departitions from membrane. The resulting loss of fluorescence provides a measure of exocytosis (Henkel et al., 1996). However, there is no significant route of exit for FM1-43 that enters the cytoplasm through a channel. Cytoplasmic dye can partition into the inner leaflet of the plasmalemma or the outer leaflet of vesicular compartments, but neither is exposed to the external milieu by exocytosis. FM1-43 could pass back out through a channel, but the inward driving force on the divalent cation would make the efflux negligible. Thus, a hallmark and third advantage of FM1-43 loading through ion channels is its persistence. We see little reduction of cytoplasmic fluorescence in hair cells when FM1-43 is washed out from the bath, and FM1-43 is retained in long-term cultures of hair cell epithelia for at least 21 d. Similarly, after a single injection of FM1-43, bright fluorescence is retained *in vivo* in the sensory cells and neurons for at least 2 weeks *in vivo*.

Additionally, this technique is unique for its specificity. With a single injection of dye, at least 10 classes of sensory cells become brightly labeled, whereas surrounding tissues remain unlabeled. This provides resolvability of individual sensory cell somata, processes, and terminals throughout the body. Most other cell-labeling techniques are less specific and require either focal applications to reduce generalized staining (e.g., DiI), or specific targeting based on genetic analysis (e.g., GFP). With styryl dyes, specific systems can be examined by focal injection or application *in vitro* or dye can be given systemically for broad examination of sensory systems. Furthermore, injections can be done far from the cells of study, the dye is nontoxic, and the labeling requires no external stimulation or manipulation of the cells, so styryl dyes present an opportunity to visualize cells and sensory transduction under normal *in vivo* conditions with minimal disruption to the cells.

A final, significant advantage of this labeling technique is that it provides an optical measure of ion channel function, because closed or nonfunctional channels do not pass FM1-43. Therefore, styryl dyes can be used to screen for mutations affecting sensory transduction in sensory systems *in vivo* and in cloned channels *in vitro*. Additionally, they can be used as an *in vitro* or *in vivo* assay for compounds that block or stimulate sensory transduction channels, including novel anesthetics or anti-nociceptive drugs. Thus, the use of styryl dyes in may greatly accelerate our understanding about the mechanisms and genetics of sensory transduction.

References

Assad JA, Shepherd GM, Corey DP (1991) Tip-link integrity and mechanical transduction in vertebrate hair cells. Neuron 7:985–994.

Balak KJ, Corwin JT, Jones JE (1990) Regenerated hair cells can originate from supporting cell progeny: evidence from phototoxicity and laser ablation experiments in the lateral line system. J Neurosci 10:2502–2512.

Baumann KI, Haman W, Leung MS (1990) Acute effects of neomycin on slowly adapting type I and type II cutaneous mechanoreceptors in the anaesthetized cat and rat. J Physiol (Lond) 425:527–544.

Betz WJ, Mao F, Smith CB (1996) Imaging exocytosis and endocytosis. Curr Opin Neurobiol 6:365–371.

Brandle U, Zenner HP, Ruppersberg JP (1999) Gene expression of P2X-receptors in the developing inner ear of the rat. Neurosci Lett 273:105–108.

Caterina MJ, Schumacher MA, Tominaga M, Rosen TA, Levine JD, Julius D (1997) The capsaicin receptor: a heat-activated ion channel in the pain pathway. Nature 389:816–824.

Collazo A, Fraser SE, Mabee PM (1994) A dual embryonic origin for vertebrate mechanoreceptors. Science 264:426–430.

Corey DP, Hudspeth AJ (1979) Ionic basis of the receptor potential in a vertebrate hair cell. Nature 281:675–677.

Corey DP, Hudspeth AJ (1983) Kinetics of the receptor current in bullfrog saccular hair cells. J Neurosci 3:962–976.

Diamond J, Holmes M, Nurse CA (1986) Are Merkel cell-neurite reciprocal synapses involved in the initiation of tactile responses in salamander skin? J Physiol (Lond) 376:101–120.

Forge A, Richardson G (1993) Freeze fracture analysis of apical membranes in cochlear cultures: differences between basal and apical-coil outer hair cells and effects of neomycin. J Neurocytol 22:854–867.

Gale JE, Marcotti W, Kennedy HJ, Kros CJ, Richardson GP (2001) FM1-43 dye behaves as a permeant blocker of the hair cell mechanotransducer channel. J Neurosci 21:7013–7025.

Garcia-Martinez C, Morenilla-Palao C, Planells-Cases R, Merino JM, Ferrer-Montiel A (2000) Identification of an aspartic residue in the P-loop of the vanilloid receptor that modulates pore properties. J Biol Chem 275:32552–32558.

Gilbertson TA, Damak S, Margolskee RF (2000) The molecular physiology of taste transduction. Curr Opin Neurobiol 10:519–527.

Griesinger CB, Richards CD, Ashmore JF (2002) FM1-43 reveals membrane recycling in adult inner hair cells of the mammalian cochlea. J Neurosci 22:3939–3952.

Hasson T, Gillespie PG, Garcia JA, MacDonald RB, Zhao Y, Yee AG, Mooseker MS, Corey DP (1997) Unconventional myosins in inner-ear sensory epithelia. J Cell Biol 137:1287–1307.

Henkel AW, Lubke J, Betz WJ (1996) FM1-43 dye ultrastructural localization in and release from frog motor nerve terminals. Proc Natl Acad Sci USA 93:1918–1923.

Hille B (1971) The permeability of the sodium channel to organic cations in myelinated nerve. J Gen Physiol 58:599–619.

Hille B (1992) Ionic channels of excitable membranes. Sunderland, MA: Sinauer.

Holt JR, Corey DP, Eatock RA (1997) Mechanoelectrical transduction and adaptation in hair cells of the mouse utricle, a low-frequency vestibular organ. J Neurosci 17:8739–8748.

Housley GD, Kanjhan R, Raybould NP, Greenwood D, Salih SG, Jarlebark L, Burton LD, Setz VC, Cannell MB, Soeller C, Christie DL, Usami S, Matsubara A, Yoshie H, Ryan AF, Thorne PR (1999) Expression of the P2X(2) receptor subunit of the ATP-gated ion channel in the cochlea: implications for sound transduction and auditory neurotransmission, J Neurosci 19:8377–8388.

Huang CJ, Favre I, Moczydlowski E (2000) Permeation of large tetraalkylammonium cations through mutant and wild-type voltage-gated sodium channels as revealed by relief of block at high voltage. J Gen Physiol 115:435–454.

Iggo A, Muir AR (1969) The structure and function of a slowly adapting touch corpuscle in hairy skin. J Physiol (Lond) 200:763–796.

Ikeda I, Yamashita Y, Ono T, Ogawa H (1994) Selective phototoxic destruction of rat Merkel cells abolishes responses of slowly adapting type I mechanoreceptor units. J Physiol (Lond) 479:247–256.

Ishida Y, Ugawa S, Ueda T, Murakami S, Shimada S (2002) Vanilloid receptor subtype-1 (VR1) is specifically localized to taste papillae. Mol Brain Res 107:17–22.

Jarlebark LE, Housley GD, Thorne PR (2000) Immunohistochemical localization of adenosine 5′-triphosphate-gated ion channel P2X(2) receptor subunits in adult and developing rat cochlea. J Comp Neurol 421:289–301.

Jorgensen F (1989) Evolution of octavolateralis sensory cells. In: The mechanosensory lateral line: neurobiology and evolution (Coombs PGS, Muenz H, eds), pp 115–145. New York: Springer.

Kachar B, Battaglia A, Fex J (1997) Compartmentalized vesicular traffic around the hair cell cuticular plate. Hear Res 107:102–112.

Khakh BS, Bao XR, Labarca C, Lester HA (1999) Neuronal P2X transmitter-gated cation channels change their ion selectivity in seconds. Nat Neurosci 2:322–330.

Kimitsuki T, Nakagawa T, Hisashi K, Komune S, Komiyama S (1996) Gadolinium blocks mechano-electric transducer current in chick cochlear hair cells. Hear Res 101:75–80.

Liedtke W, Choe Y, Marti-Renom MA, Bell AM, Denis CS, Sali A, Hudspeth AJ, Friedman JM, Heller S (2000) Vanilloid receptor-related osmotically activated channel (VR-OAC), a candidate vertebrate osmoreceptor. Cell 103:525–535.

Lippincott-Schwartz J, Fambrough DM (1986) Lysosomal membrane dynamics: structure and interorganellar movement of a major lysosomal membrane glycoprotein. J Cell Biol 102:1593–1605.

Lumpkin EA, Marquis RE, Hudspeth AJ (1997) The selectivity of the hair cell's mechanoelectrical-transduction channel promotes Ca^{2+} flux at low Ca^{2+} concentrations. Proc Natl Acad Sci USA 94:10997–11002.

Margolskee RF (2002) Molecular mechanisms of bitter and sweet taste transduction. J Biol Chem 277:1–4.

Meyer J, Mack AF, Gummer AW (2001) Pronounced infracuticular endocytosis in mammalian outer hair cells. Hear Res 161:10–22.

Michael GJ, Priestley JV (1999) Differential expression of the mRNA for the vanilloid receptor subtype 1 in cells of the adult rat dorsal root and nodose ganglia and its downregulation by axotomy. J Neurosci 19:1844–1854.

Mills LR, Diamond J (1995) Merkel cells are not the mechanosensory transducers in the touch dome of the rat. J Neurocytol 24:117–134.

Nagle JF, Tristram-Nagle S (2000) Structure of lipid bilayers. Biochim Biophys Acta 1469:159–195.

Nishikawa S, Sasaki F (1996) Internalization of styryl dye FM1-43 in the hair cells of lateral line organs in *Xenopus* larvae. J Histochem Cytochem 44:733–741.

Nurse CA, Farraway L (1989) Characterization of Merkel cells and mechanosensory axons of the rat by styryl pyridinium dyes. Cell Tissue Res 255:125–128.

Ohmori H (1985) Mechanoelectrical transduction currents in isolated vestibular hair cells of the chick. J Physiol (Lond) 359:189–217.

Osborne MP, Comis SD (1990) Action of elastase, collagenase and other enzymes upon linkages between stereocilia in the guinea-pig cochlea. Acta Otolaryngol 110:37–45.

Pacitti EG, Findlater GS (1988) Calcium channel blockers and Merkel cells. Prog Brain Res 74:37–42.

Perez CA, Huang L, Rong M, Kozak JA, Preuss AK, Zhang H, Max M, Margolskee RF (2002) A transient receptor potential channel expressed in taste receptor cells. Nat Neurosci 5:1169–1176.

Periasamy N, Verkman AS (1998) Analysis of fluorophore diffusion by continuous distributions of diffusion coefficients: application to photobleaching measurements of multicomponent and anomalous diffusion. Biophys J 75:557–567.

Ryan TA, Smith SJ, Reuter H (1996) The timing of synaptic vesicle endocytosis. Proc Natl Acad Sci USA 93:5567–5571.

Schaeffer SF, Raviola E (1978) Membrane recycling in the cone cell endings of the turtle retina. J Cell Biol 79:802–825.

Schote U, Seelig J (1998) Interaction of the neuronal marker dye FM1-43 with lipid membranes. Thermodynamics and lipid ordering. Biochim Biophys Acta 1415:135–146.

Seiler C, Nicolson T (1999) Defective calmodulin-dependent rapid apical endocytosis in zebrafish sensory hair cell mutants. J Neurobiol 41:424–434.

Self T, Sobe T, Copeland NG, Jenkins NA, Avraham KB, Steel KP (1999) Role of myosin VI in the differentiation of cochlear hair cells. Dev Biol 214:331–341.

Senok SS, Baumann KI (1997) Functional evidence for calcium-induced calcium release in isolated rat vibrissal Merkel cell mechanoreceptors. J Physiol (Lond) 500:29–37.

Shepherd GMG, Corey DP (1994) The extent of adaptation in bullfrog saccular hair cells. J Neurosci 14:6217–6229.

Shepherd GMG, Barres BA, Corey DP (1989) "Bundle Blot" purification and initial protein characterization of hair cell stereocilia. Proc Natl Acad Sci USA 86:4973–4977.

Virginio C, MacKenzie A, Rassendren FA, North RA, Surprenant A (1999) Pore dilation of neuronal P2X receptor channels. Nat Neurosci 2:315–321.

Walker RG, Willingham AT, Zuker CS (2000) A *Drosophila* mechanosensory transduction channel. Science 287:2229–2234.

Xiang Z, Bo X, Burnstock G (1998) Localization of ATP-gated P2X receptor immunoreactivity in rat sensory and sympathetic ganglia. Neurosci Lett 256:105–108.

Xiang Z, Bo X, Burnstock G (1999) P2X receptor immunoreactivity in the rat cochlea, vestibular ganglion and cochlear nucleus. Hear Res 128:190–196.

Xu H, Ramsey IS, Kotecha SA, Moran MM, Chong JA, Lawson D, Ge P, Lilly J, Silos-Santiago I, Xie Y, DiStefano PS, Curtis R, Clapham DE (2002) TRPV3 is a calcium-permeable temperature-sensitive cation channel. Nature 418:181–186.

Zenisek D, Steyer JA, Feldman ME, Almers W (2002) A membrane marker leaves synaptic vesicles in milliseconds after exocytosis in retinal bipolar cells. Neuron 35:1085–1097.

Zhang Y, Hoon MA, Chandrashekar J, Mueller KL, Cook B, Wu D, Zuker CS, Ryba NJP (2003) Coding of sweet, bitter, and umami tastes: different receptor cells sharing similar signaling pathways. Cell 112:293–301.